ARTICLE

Hydrogen Bonding Effects on the Photophysical Properties of 2,3-dihydro-3-keto-1H-pyrido[3,2,1-kl]phenothiazine

Song-qiu Yang[a,b*], Guo-zhong He[a]

a. State Key Laboratory of Molecular Reaction Dynamics, Dalian Institute of Chemical Physics, Chinese Academy of Sciences, Dalian 116023, China
b. Graduate School of the Chinese Academy of Sciences, Beijing 100039, China

(Dated: Received on February 20, 2012; Accepted on March 16, 2012)

Time-dependent density functional theory (TDDFT) and femtosecond transient absorption spectroscopy were used to investigate the photophysical properties of 2,3-dihydro-3-keto-1H-pyrido[3,2,1-kl]phenothiazine (PTZ4) and 3-keto-1H-pyrido[3,2,1-kl]phenothiazine (PTZ5). The calculated results obtained from TDDFT suggest that the red-shifts of the absorption spectra of these two fluorophores in methanol are due to the formation of hydrogen-bonded complexes at the ground state. Four conformers of PTZ4 were obtained by TDDFT. The two fluorescence peaks of PTZ4 in tetrahydrofuran (THF) came from the ICT states of the four conformers. The fluorescence of PTZ4 in THF showed a dependence on the excitation wavelength because of butterfly bending. The excited state dynamics of PTZ4 in THF and methanol were obtained by transient absorption spectroscopy. The lifetime of the excited PTZ4 in methanol was 53.8 ps, and its relaxation from the LE state to the ICT state was completed within several picoseconds. The short lifetime of excited PTZ4 in methanol was due to the formation of out-of-plane model hydrogen bonds between PTZ4 and methanol at the excited state.

Key words: 2,3-dihydro-3-keto-1H-pyrido[3,2,1-kl]phenothiazine, Time-dependent density functional theory, Femtosecond transient absorption spectroscopy, Hydrogen bonding effect

I. INTRODUCTION

The photophysical properties of fluorophores in different solvent environments have been investigated intensively [1]. The fluorescence of fluorophores is quenched or enhanced by changes in the solvent environment and by the formation of hydrogen bonds between the fluorophore and solvent molecules. The excited-state intra- and intermolecular proton transfer reactions are considered as a fundamental and important process in the excited-state dynamics of fluorophores [2−8]. Lim established the "proximity effect" theory to understand the enhanced fluorescence of nitrogen-heterocyclic and aromatic carbonyl compounds in alcohols [9]. Yatsuhashi and co-workers believed that the formation of out-of-plane hydrogen bonds between fluorophores and alcohols plays an important role in non-emission decay [10−12]. Some researchers have also upheld the belief that butterfly bending is an effective non-emission decay pathway [13−17]. Some others found that proton transfer is not a deactivating mechanism of the excited state of some natural bases [4, 18−20]. However, for many fluorophores, proton transfer during the excited state is still an effective nonradiative process [3, 21]. Over the past few years, many studies have been done by our group to clarify the effects of hydrogen bonding on the excited-state dynamics of fluorophores, and we have obtained interesting results [22−28].

Han *et al.* recently reported several phenothiazine derivative dyes as environment-sensitive fluorescence probes [29], finding that 2,3-dihydro-3-keto-1H-pyrido[3,2,1-kl]phonothiazine (PTZ4) and 3-keto-1H-pyrido[3,2,1-kl]phenothiazine (PTZ5) have similar fluorescence intensities in aprotic solvents. However, the fluorescence of PTZ4 was quenched, whereas that of PTZ5 was enhanced in protic solvents. Theoretical investigations on the photophysical properties of PTZ5 in different solvents have been previously reported [24]. We found that the enhanced fluorescence of PTZ5 in polar protic solvents is due to the larger energy gap between the lowest two-singlet excited states and inhibition of the out-of-plane bending of C−H by the formation of hydrogen-bonded complexes [24].

In this work, to understand the mechanism of fluorescence quenching of PTZ4 in protic solvents, we measured the steady-state emission and absorption spectra, as well as the femtosecond time-resolved transient absorption spectra of PTZ4 and PTZ5 in tetrahydrofuran (THF) and methanol. Density functional theory (DFT)

*Author to whom correspondence should be addressed. E-mail: sqyang@dicp.ac.cn

and time-dependent density functional theory (TDDFT) methods were employed to calculate the optimized geometries of the ground state (S_0) and the first-singlet excited state (S_1). Transient absorption results showed the excited-state dynamics.

II. EXPERIMENTS

Transient absorption signals were recorded through the pump-probe technique using a femtosecond laser system as described previously [30]. Briefly, a Ti:sapphire femtosecond laser (Hurricane, Spectra-Physics) was used as a light source. The output power was 800 mW, with a repetition rate of 1 kHz and a pulse width of ∼130 fs. An optical parametric amplifier was used to change the laser wavelength. Pump pulses with a center wavelength of 400 nm were generated from 800 nm laser pulse by frequency doubling with a BBO crystal. A white-light continuum of the probe pulses was generated by focusing an 800 nm laser pulse (20 μJ/pulse) onto a 2 mm thick sapphire window. The white-light beam was separated into two parts: the first acted as the reference beam and the other acted as the probe beam. These beams were dispersed using a monochromator (SR-303i-A, ANDOR) and then recorded using a charge-coupled device (DV420-BV, ANDOR).

The probe beam was focused and overlapped with the pump beam, which had a spot size of 0.2 mm on the sample. Polarization of the probe beam with respect to the polarization of the pump beam was adjusted to the magic angle to avoid reorientation effects. Transient temporal decay profiles were fitted using the convolution between the instrumental response function (IRF) with a multi-exponential function and according to iterative deconvolution based on the Levenberg-Marquardt algorithm. IRF was determined using the optical Kerr effect of the *n*-hexane, as reported by Quan *et al.* [31].

The sample was placed in a flowing 1 mm cell to avoid damage. The absorption spectra of samples were obtained before and after the experiment and no changes were found. All experiments were performed at room temperature (295 K).

PTZ4 and PTZ5 were obtained as reported [29]. The concentration of PTZ5 in methanol and THF was 30 μmol/L, while that of PTZ4 was 50 μmol/L. Methanol and THF were of high-performance liquid chromatography grade and subjected to no additional treatment. THF and methanol were chosen in our experiment and calculations because of their similar polarities.

UV-Vis absorption spectra were obtained using a Perkin-Elmer Lambda 35 double-beam spectrometer. Fluorescence spectra were recorded with a JASCO FP-6500 spectrometer and Sanco 970CRT fluorospectrometer.

III. COMPUTATIONAL DETAILS

DFT/TDDFT calculations were carried out with the Gaussian 09 program [32]. The geometry optimizations of the ground state and excited states were performed using DFT/TDDFT methods. The B3LYP functional was employed. The B3LYP/6-31G(d,p) level is satisfactory for calculating the ground-state and excited-state optimized geometries of PTZ4 and PTZ5. The larger basis set obtained little improvement but time consumer. Therefore, the standard 6-31G(d,p) split-valance double-zeta basis set with polarization functions for all atoms was used in the geometry optimization of S_0 and S_1. Following each optimization, the vibrational frequencies were computed, and all vibrational frequencies were real. Vertical excited energies were calculated at optimized geometries using TDDFT method. Calculations considering solvent effects were performed in the presence of a solvent by placing the solute in a cavity within the solvent reaction field (SCRF). The conductor-like polarizable continuum model (CPCM) was used in SCRF.

IV. RESULTS AND DISCUSSION

Steady-state absorption and fluorescence spectra were previously reported by Han *et al.* [29]. In this work, some steady-state spectra were recorded in detail for better discussion. Figure 1 (a) and (b) show the absorption spectra of PTZ4 and PTZ5 in THF and methanol. The absorption spectra of these two dyes evidently shifted to longer wavelengths in methanol than in THF. These redshifts in absorption spectra may be induced by the formation of hydrogen-bonded complexes in methanol.

Given the flexibility of the N−C15−C16−C17 structure, four conformers of PTZ4 were optimized by TDDFT at S_0. Figure 2 shows these four geometries: A, B, C, and D. A and B are symmetric conformers, as are C and D are also symmetric conformers. For simplification, we only studied the photophysical properties of A and C because symmetric conformers have similar photophysical properties, the calculation results of B and D are not shown here. Conformer A is more stable than conformer C at S_0 by 15.88 kJ/mol. Thus, conformers A and B are the major conformers in the solutions. The S_1 vertical excited energy of conformer A at the S_0-optimized geometry in THF is 2.9456 eV (Table I).

Hydrogen-bonded complexes were formed when PTZ4 was dissolved in methanol. According to previous reports, we know that the secondary hydrogen bond between C−H and oxygen is an important factor that influences the excited-state dynamics of fluorophores [24]. Considering that there are two C16−H bonds in PTZ4, two methanol molecules were added to form hydrogen-bonded complexes with PTZ4 (Fig.3, A-2MeOH). One methanol formed a hydrogen bond with

DOI:10.1088/1674-0068/25/03/254-260

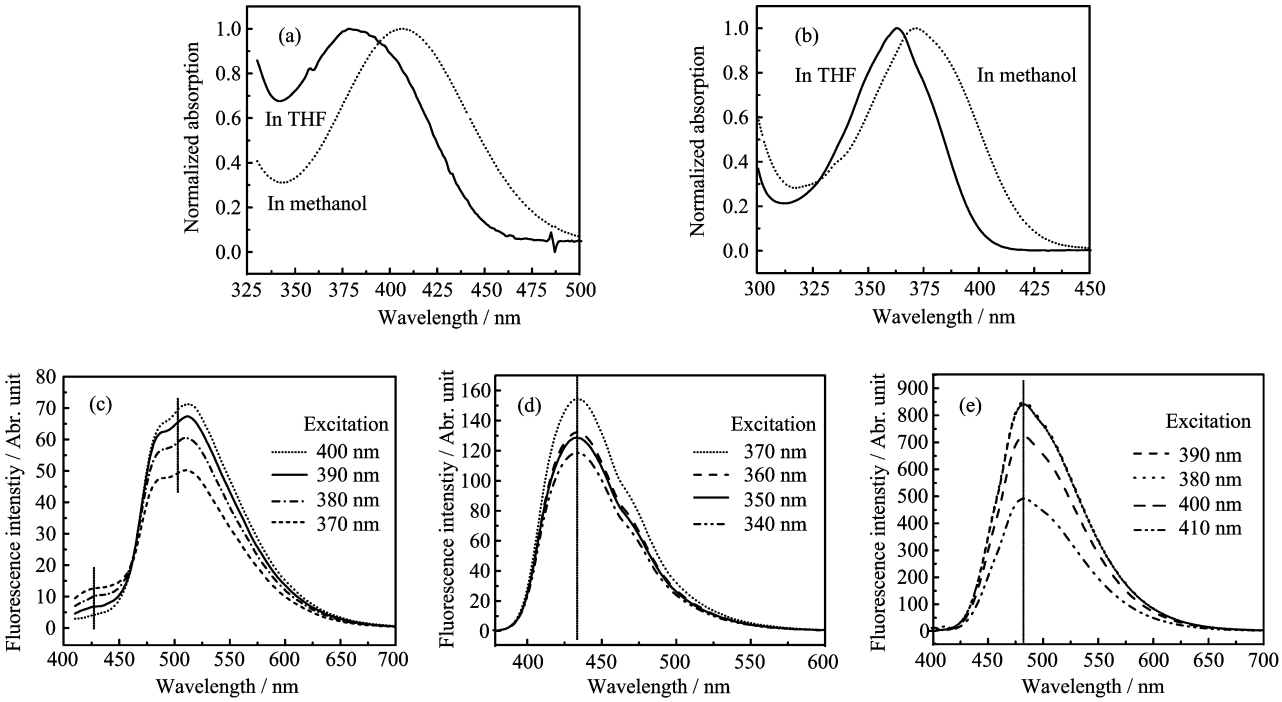

FIG. 1 Steady-state absorption and fluorescence spectra of PTZ4 and PTZ5 in THF and methanol. (a) Absorption spectra of PTZ4 in THF and methanol. (b) Absorption spectra of PTZ5 in THF and methanol. (c) Fluorescence spectra of PTZ4 in THF measured at different excitation wavelengths. (d) Fluorescence spectra of PTZ5 in THF. (e) Fluorescence spectra of PTZ5 in methanol.

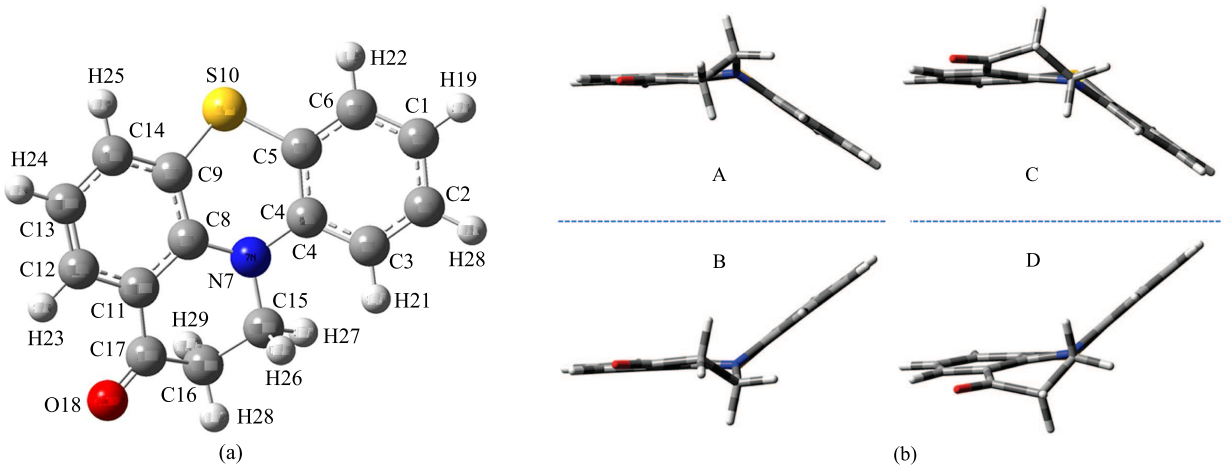

FIG. 2 The geometries of PTZ4 and its four conformers. A and B are symmetric conformers, C and D are also symmetric conformers.

O18 in plane mode, and another methanol formed a hydrogen bond with O18 in the out-of-plane mode approaching the p_z orbital (Fig.3) [10]. The S_1 vertical excited energy of A-2MeOH calculated at the S_0-optimized geometry was 2.6402 eV. As reported previously, the S_1 vertical excited energies of PTZ5 (in THF) and PTZ5-MeOH are 3.5081 and 3.4120 eV, respectively [24]. These results indicate the redshift in absorption spectra from THF to methanol. Therefore, redshifts in the absorption spectra of PTZ4 and PTZ5 are due to the formation of hydrogen-bonded complexes at each S_0 in methanol. The calculations considered solvation effects in the CPCM model. The calculated vertical excited energies of conformers A and C and their hydrogen-bonded complexes at the S_0-optimized geometry are shown in Table I.

The fluorescence spectra of PTZ4 in THF and PTZ5 in THF and methanol were obtained at different excitation wavelengths and are shown in Fig.1. The emission rate constants k_f of PTZ5 showed no significant

DOI:10.1088/1674-0068/25/03/254-260

TABLE I Characteristic structures of PTZ4 at S_0- and S_1-optimized geometries. These results were calculated at the B3LYP/6-31G(d, p) level. Solvation effects were considered in the CPCM model. A and C indicate the conformers of PTZ4. A-2MeOH is the hydrogen bonded complex of PTZ4 with two methanols.

Geometry	Conformer	Solvent	∠N7C15C16C17/(°)	∠C5C4N7C8/(°)	S_1/eV	$L_{H31\cdots O18}$/pm	$L_{H37\cdots O18}$/pm
S_0-opt	A	THF	−55.47	38.66	2.9456		
	C	THF	56.58	34.68	3.0515		
	A-2MeOH	MeOH	−52.11	37.66	2.6400	191.14	200.21
S_1-opt	A	THF	−53.10	21.91	2.2315		
	C	THF	49.56	16.34	2.2705		
	A-2MeOH	MeOH	−50.64	22.48	1.8381	176.42	177.05

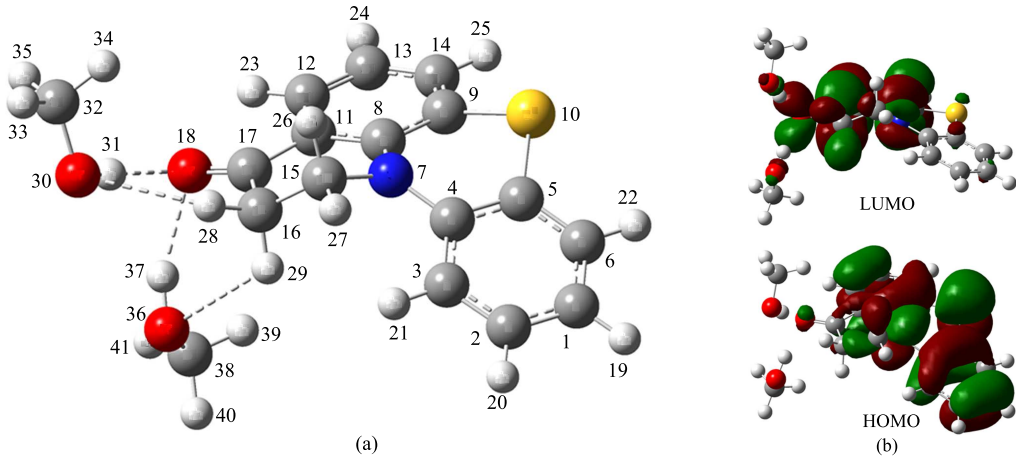

FIG. 3 (a) The geometry of PTZ5 at the S_0-optimized geometry. (b) The relevant frontier molecular orbitals of PTZ5 at the S_1-optimized geometry.

changes in various solvents [29]. In addition, the emission state of PTZ5 was always the bright state (π, π^*) [24]. Figures 1 (d) and (e) show that the fluorescence spectra of PTZ5 in THF and methanol are independent of the excitation wavelength. Only one relaxed emission state exists, as results suggest, which is consistent with the findings in previous studies [24, 29]. Larger Stoks shifts more in fluorescence for PTZ5 in methanol than in THF, which may be due to enhanced hydrogen bonds at the optimized S_1. The calculated results show that the O−H−O=C hydrogen bond length is 190.7 pm for PTZ5-MeOH at the S_0-optimized geometry and 180.6 pm at the S_1-optimized geometry.

The fluorescence spectra of PTZ4 in THF show two peaks at approximately 490 and 510 nm (Fig.1(c)). We believe that these two proximity fluorescent peaks are not due to the vibrational structure. Instead, the peaks may come from the relaxed emission states of PTZ4, because the fluorescence intensity at the 490 and 510 nm peaks shows some dependence on the excitation wavelength (Fig.1(c)). TDDFT calculations validate our proposal. Table I shows the vertical excited energies of PTZ4 conformers A and C in THF at S_1-optimized geometries. The emission from conformer A is 2.23 eV (556 nm) and that from conformer C is 2.27 eV (546 nm). Although the calculated vertical energies are lower than the experimental results, two emission states actually exist for PTZ4. Therefore, assigning the 490 nm peak to conformer C and the 510 nm peak to conformer A is reasonable. The large Stoks shift and relative molecular orbitals suggest that these two proximal relaxed emission states are internal-charge transfer (ICT) states [24, 29]. In addition, the low fluorescence peak at approximately 430 nm can be assigned to the local excited (LE) state. The fluorescence of PTZ4 in methanol was quenched entirely (data not shown).

Some characteristic structures of conformers A and C are shown in Table I. From the dihedral angle of C5C4NC8 at S_0- and S_1-optimized geometries (38.66° and 21.91°, respectively), S_1-optimized geometries are clearly more planar than S_0 geometries. Therefore, relaxation from the Franck-Condon state to ICT states may be induced by butterfly bending. Butterfly bending is generally thought to be an important nonradiative decay pathway [13−17]. Thus, the excitation wavelength dependence of the PTZ4 emission spectra could be induced by butterfly bending.

According to the discussions above, an excited-state relaxation model was proposed, as shown in Fig.4. The key excited states along the excited-state relaxation path are shown: the LE state, ICT states, and hydrogen-bonded complex emission states. In apro-

DOI:10.1088/1674-0068/25/03/254-260

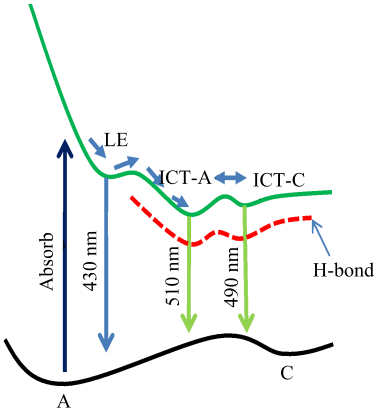

FIG. 4 Excited-state relaxation model for excited PTZ4. The dashed line indicates the potential energy surface of PTZ4 in protic solvents. ICT-A: the ICT state of conformer A. ICT-C: the ICT state of conformer C.

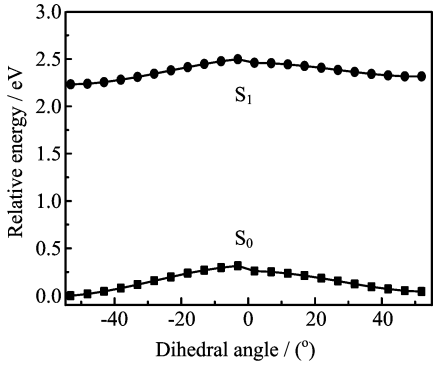

FIG. 5 Minimum energy profile of S_1 along the change in dihedral angle of NC15C16C17 from $-52°$ to $52°$ for PTZ4 in THF. The S_0 energy at conformer A the S_1-optimized geometry of conformer A was set to zero.

tic solvents, the populations of PTZ4 at the Franck-Condon state first relaxed to the LE state and then relaxed quickly to two ICT states. An equilibrium is built up between the two ICT states at the excited-state potential energy surface with a barrier of 0.27 eV in THF (Fig.5).

The femtosecond transient absorption spectroscopy method was used to measure the excited-state dynamics of PTZ4 in methanol and THF. Figure 6 shows the results obtained from transient absorption spectroscopy. From 450 nm to 710 nm, only one large excited-state absorption (ESA) peak for PTZ4 was observed both in methanol and in THF. Figure 6 (a) and (b) show that the ESA peak shifted from 590 nm to 560 nm in THF. Figure 6 (c) and (d) show that the peak of ESA shifts from 570 nm to 545 nm in methanol. It is well known that, relaxed ICT states are lower than LE states so it is reasonable to assume that the peak of ESA from the ICT state to a higher excited state is blue shift than the peak of ESA from LE state to a higher excited state. Therefore, the blue-shift in ESA peak is due to excited-state relaxation from the Franck-Condon geometry (or LE state) to the S_1-optimized geometry (ICT state) and solvation dynamics. The lack of double ESA peaks at the two ICT states may be due to the poor signal-to-noise ratio.

Typical decay profiles of the ICT states of PTZ4 in THF (565 nm) and methanol (550 nm) are shown in Fig.7. The fitted results show that the rise-time constants are 16.0 and 7.5 ps for PTZ4 in THF and methanol, respectively. These rise-time constants correspond to relaxation from the LE state to the ICT state. The S_1 of PTZ4 in methanol has a 53.8 ps lifetime. This result is consistent with the low-fluorescence quantum yields of PTZ4 in methanol [29], and the short lifetime of the excited state of PTZ4 in methanol may be induced by hydrogen-bonded complex formation.

The characteristic structures of conformer A-2MeOH at S_0- and S_1-optimized geometries are also shown in Table I. The two hydrogen bonds are all enhanced at the S_1-optimized geometry. The distance between H31 and O18 is 191.1 pm at the S_0-optimized geometry and 176.4 pm at the S_1-optimized geometry. As well, the distance between H37 and O18 is 200.2 pm at the S_0 geometry and 177.0 pm at the S_1 geometry. Interestingly, the out-of-plane mode of the hydrogen bond H37$\cdots$O18 was significantly enhanced. Out-of-plane mode attack has been reported by Yatsuhashi *et al.* [10−12], who proposed that out-of-plane mode attacks could form non-emissive hydrogen-bonded excited states. This proposal may help facilitate understanding of the short lifetime of the PTZ4 excited-state in methanol.

V. CONCLUSION

The steady-state UV-Vis absorption and fluorescence spectra of PTZ4 and PTZ5 in THF and methanol were investigated. TD-DFT calculated results reveal that redshifts in absorption spectra of PTZ4 and PTZ5 in methanol were due to the formation of hydrogen-bonded complexes at S_0. The fluorescence spectra of PTZ5 are independent of the excitation wavelength, suggesting that only one relaxed emission excited state exists. The two fluorescence peaks of PTZ4 in THF are assigned to the ICT states of the four conformers A and B, and C and D. The small fluorescence peak at 430 nm is due to emissions from the LE states. The calculated results suggest that, along with the LE state changing to the ICT state, PTZ4 undergoes butterfly bending, which may contribute to the dependence of fluorescence on the excitation wavelengths. The dynamics of LE to ICT states was measured by transient absorption spectroscopy. Relaxation from the LE state to the ICT state yielded 16.0 and 7.5 ps time constants for PTZ4 in THF and methanol, respectively. The lifetime of excited PTZ4 in methanol is 53.8 ps. This short lifetime of PTZ4 in methanol is due to the formation of

DOI:10.1088/1674-0068/25/03/254-260

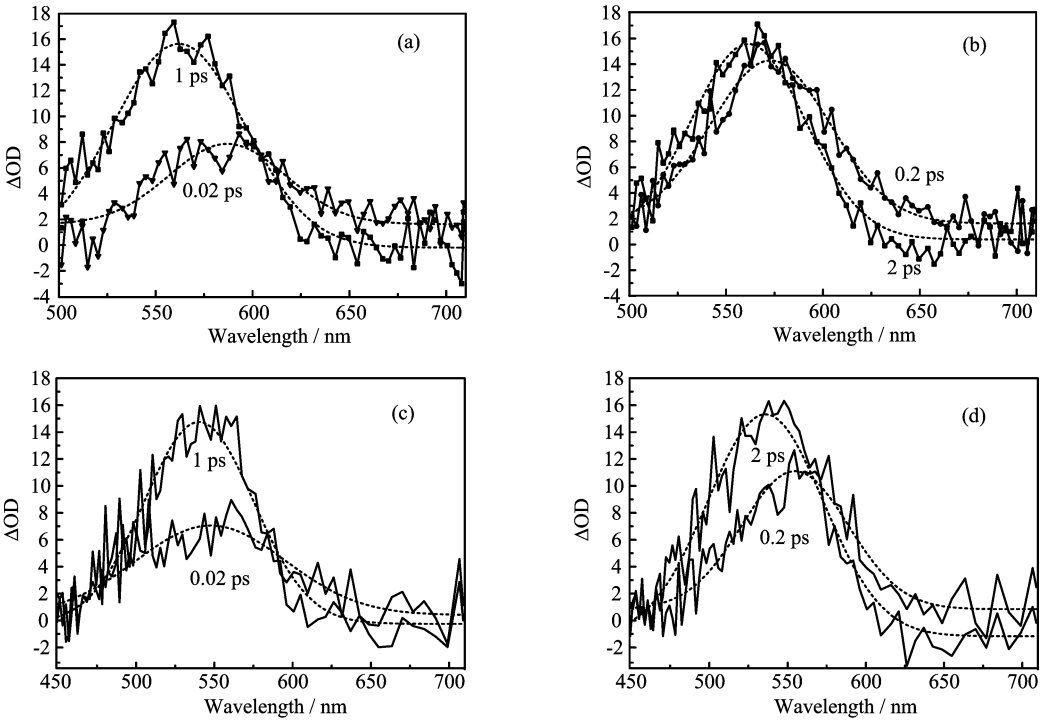

FIG. 6 Transient absorption results of PTZ4 in THF ((a) and (b)) and methanol ((c) and (d)). The broken line are fitted results. The pump is 400 nm and the probe is continuum white light.

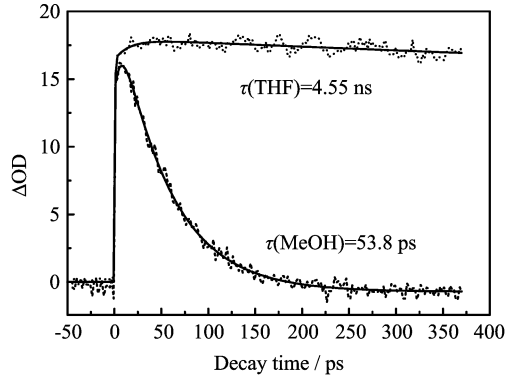

FIG. 7 Character decay profiles obtained from transient absorption spectroscopy of PTZ4 in methanol and THF. The solid line are fitted result. The decay time constant τ(THF)=4.55 ns was cited from Ref.[29].

out-of-plane model hydrogen-bonded complexes.

VI. ACKNOWLEDGMENTS

We thank Professor Jian-zhang Zhao for providing samples and helpful discussion. This work was supported by the National Natural Science Foundation of China (No.20973168).

[1] J. R. Lakowicz, *Principles of Fluorescence Spectroscopy*, 3rd Edn., New York: Springer Science+Business Media, LLC, (2006).
[2] C. C. Hsieh, C. M. Jiang, and P. T. Chou, Accounts Chem. Res. **43**, 1364 (2010).
[3] J. E. Kwon and S. Y. Park, Advanced Materials **23**, 3615 (2011).
[4] C. E. Crespo-Hernandez, B. Cohen, P. M. Hare, and B. Kohler, Chem. Rev. **104**, 1977 (2004).
[5] Y. F. Liu, Y. G. Yang, K. Jiang, D. H. Shi, and J. F. Sun, Bull. Chem. Soc. Jpn. **84**, 191 (2011).
[6] X. H. Zhao and M. D. Chen, J. Phys. Chem. A **114**, 7786 (2010).
[7] H. F. Wang, M. S. Wang, E. F. Liu, M. L. Xin, and C. L. Yang, Comput. Theor. Chem **964**, 243 (2011).
[8] H. F. Wang, M. S. Wang, M. L. Xin, E. F. Liu, and C. L. Yang, Centr. Eur. J. Phys. **9**, 792 (2011).
[9] E. C. Lim, J. Phys. Chem. **90**, 6770 (1986).
[10] T. Yatsuhashi and H. Inoue, J. Phys. Chem. A **101**, 8166 (1997).
[11] T. Yatsuhashi, Y. Nakajima, T. Shimada, and H. Inoue, J. Phys. Chem. A **102**, 3018 (1998).
[12] T. Yatsuhashi, Y. Nakajima, T. Shimada, H. Tachibana, and H. Inoue, J. Phys. Chem. A **102**, 8657 (1998).
[13] B. W. Lennon, C. H. Williams, and M. L. Ludwig, Protein Sci. **8**, 2366 (1999).
[14] Y. J. Zheng and R. L. Ornstein, J. Am. Chem. Soc. **118**, 9402 (1996).
[15] Y. T. Kao, C. Saxena, T. F. He, L. J. Guo, L. J. Wang, A. Sancar, and D. P. Zhong, J. Am. Chem. Soc. **130**,

DOI:10.1088/1674-0068/25/03/254-260

13132 (2008).
[16] Y. T. Kao, C. Tan, S. H. Song, N. Ozturk, J. Li, L. J. Wang, A. Sancar, and D. P. Zhong, J. Am. Chem. Soc. **130**, 7695 (2008).
[17] O. Rubio-Pons, L. Serrano-Andres, D. Burget, and P. Jacques, J. Photochem. Photobiol. A **179**, 298 (2006).
[18] B. Cohen, P. M. Hare, and B. Kohler, J. Am. Chem. Soc. **125**, 13594 (2003).
[19] L. Blancafort, B. Cohen, P. M. Hare, B. Kohler, and M. A. Robb, J. Phys. Chem. A **109**, 4431 (2005).
[20] L. Biemann, S. A. Kovalenko, K. Kleinermanns, R. Mahrwald, M. Markert, and R. Improta, J. Am. Chem. Soc. **133**, 19664 (2011).
[21] A. Sinicropi, W. M. Nau, and M. Olivucci, Photochem. Photobiol. Sci. **1**, 537 (2002).
[22] G. J. Zhao and K. L. Han, J. Phys. Chem. A **111**, 9218 (2007).
[23] K. L. Han and G. J. Zhao, *Hydrogen Bonding and Transfer in the Excited State*, New York: John Wiley & Sons, Ltd., Vol.1−2, (2010).
[24] S. Q. Yang, J. Y. Liu, P. W. Zhou, and G. Z. He, J. Phys. Chem. B **115**, 10692 (2011).
[25] G. J. Zhao and K. L. Han, J. Comput. Chem. **29**, 2010 (2008).
[26] S. Chai, G. J. Zhao, P. Song, S. Q. Yang, J. Y. Liu, and K. L. Han, Phys. Chem. Chem. Phys. **11**, 4385 (2009).
[27] P. W. Zhou, P. Song, J. Y. Liu, K. L. Han, and G. Z. He, Phys. Chem. Chem. Phys. **11**, 9440 (2009).
[28] G. Y. Li, G. J. Zhao, Y. H. Liu, K. L. Han, and G. Z. He, J. Comput. Chem **31**, 1759 (2010).
[29] F. Han, L. Chi, W. Wu, X. Liang, M. Fu, and J. Zhao, J. Photochem. Photobiol. A **196**, 10 (2008).
[30] S. Q. Yang, J. Y. Liu, P. W. Zhou, K. L. Han, and G. Z. He, Chem. Phys. Lett. **512**, 66 (2011).
[31] D. Quan, S. Liu, L. Zhang, J. Yang, L. Wang, G. Yang, and Y. Weng, Chin. Phys. **12**, 986 (2003).
[32] M. J. Frisch, G. W. Trucks, H. B. Schlegel, G. E. Scuseria, M. A. Robb, J. R. Cheeseman, G. Scalmani, V. Barone, B. Mennucci, G. A. Petersson, H. Nakatsuji, M. Caricato, X. Li, H. P. Hratchian, A. F. Izmaylov, J. Bloino, G. Zheng, J. L. Sonnenberg, M. Hada, M. Ehara, K. Toyota, R. Fukuda, J. Hasegawa, M. Ishida, T. Nakajima, Y. Honda, O. Kitao, H. Nakai, T. Vreven, J. A. Montgomery, J. E. P. Jr., F. Ogliaro, M. Bearpark, J. J. Heyd, E. Brothers, K. N. Kudin, V. N. Staroverov, R. Kobayashi, J. Normand, K. Raghavachari, A. Rendell, J. C. Burant, S. S. Iyengar, J. Tomasi, M. Cossi, N. Rega, J. M. Millam, M. Klene, J. E. Knox, J. B. Cross, V. Bakken, C. Adamo, J. Jaramillo, R. Gomperts, R. E. Stratmann, O. Yazyev, A. J. Austin, R. Cammi, C. Pomelli, J. W. Ochterski, R. L. Martin, K. Morokuma, V. G. Zakrzewski, G. A. Voth, P. Salvador, J. J. Dannenberg, S. Dapprich, A. D. Daniels, O. Farkas, J. B. Foresman, J. V. Ortiz, J. Cioslowski, and D. J. Fox, *Gaussian 09, Revision A.02*, Wallingford CT: Gaussian, Inc., (2009).

DOI:10.1088/1674-0068/25/03/254-260